JOURNAL OF CATALYSIS **62**, 235–242 (1980)

Mechanism and Structure Sensitivity of Propane Hydrogenolysis over Ni/SiO$_2$ Catalysts

M. F. GUILLEUX,[1] J. A. DALMON, AND G. A. MARTIN

Institut de Recherches sur la Catalyse, 2 Avenue Albert Einstein, 69626 Villeurbanne Cédex, France

Received November 30, 1978; revised July 23, 1979

In propane hydrogenolysis two parallel reactions may occur, $C_3H_8 + H_2 = CH_4 + C_2H_6$ (Reaction 1) and $C_3H_8 + 2H_2 = 3CH_4$ (Reaction 2). The rate at low $P_{C_3H_8}/P_{H_2}$ is related to the degree of hydrogen coverage, θ_H, by equations similar to that previously observed for ethane hydrogenolysis:

$$r = k_0 P_{C_3H_8} e^{-E_0/RT}(1 - \theta_H)^X$$

with $E_0 = 14 \pm 3$ kcal/mole and $X = 17 \pm 3$ for Reaction (1), and with $E_0 = 9 \pm$ kcal/mole and $X = 24 \pm 3$ for Reaction (2). k_0 is of the same order of magnitude as ν, the number of propane molecules colliding with the nickel surface in unit time. The rate-limiting step is believed to be the irreversible formation of strongly dehydrogenated and cracked surface species on ensembles of X adjacent nickel atoms, free from adsorbed hydrogen, in competition with the reversible adsorption of hydrogen, as for ethane hydrogenolysis. The proposed mechanism is in good accordance with data on propane adsorption studied by magnetic methods, and with propane hydrogenolysis on Ni–Cu/SiO$_2$ catalysts. Most of the observed results on the structure sensitivity of propane hydrogenolysis are similar to those previously reported for ethane hydrogenolysis, and the conclusions reached in the latter case hold for propane hydrogenolysis, i.e.: (111) planes are least active, and all other surface nickel atoms are equivalent from the standpoint of activity.

I. INTRODUCTION

In previous work (*1*) it has been shown that the rate of ethane hydrogenolysis, r, can be represented by the simple kinetic equation:

$$r = k_0 P_{C_2H_6} e^{-E_0/RT} \theta_H{}^Y (1 - \theta_H)^X$$

where θ_H = degree of hydrogen coverage, k_0 is nearly equal to the number of ethane molecules colliding with the nickel surface in unit time, $E_0 = 14$ kcal/mole, $Y = -1 \pm 2$, and $X = 15 \pm 2$. The rate-limiting step was supposed to be the irreversible formation of the completely dehydrogenated and cracked surface species on an ensemble of X adjacent nickel atoms free from adsorbed hydrogen, in competition with the reversible adsorption of hydrogen.

The study of the hydrogenolysis of heavier hydrocarbons is of special interest, since two extreme possibilities can occur: (i) the molecule undergoes a total fragmentation leading to methane as the sole product, (ii) only one C–C bond is ruptured giving two hydrocarbons. The selectivity toward total fragmentation into methane depends on a number of parameters, such as the nature of the metal, its surface structure, experimental conditions (temperature, pressure). Thus, it seemed of interest to examine to what extent the model proposed for ethane hydrogenolysis is of general use and is capable of accounting for hydrogenolysis selectivities. This led us to perform a new kinetic study of propane hydrogenolysis over the Ni/SiO$_2$ catalyst previously used in the case of ethane hydrogenolysis, with the aim of determining a quantitative relation between the rate of hydrogenolysis and the degree of hydrogen coverage over the metallic surface. In addi-

---

[1] Present address: E.R 133 Laboratoire de Chimie des Solides, Université Pierre et Marie Curie, Tour 55, 4 place Jussieu, 75230 Paris Cédex 05, France.

0021-9517/80/040235-08$02.00/0

tion, the structure sensitivity previously observed in the case of ethane hydrogenolysis (*3*, *4*) was also examined for propane hydrogenolysis.

II. EXPERIMENTAL METHODS AND MATERIALS

Experiments were carried out using the same apparatus and the same samples as those previously described (*1*, *3*, *4*). Let us recall briefly that Ni/SiO_2 catalysts were obtained by reducing for 15 hr in a hydrogen stream a precursor prepared by reacting aerosil silica with a solution of nickel nitrate hexammine. The structure sensitivity of the reaction was investigated over a series of completely reduced Ni/SiO_2 catalysts in which the average nickel particle size was varied from 2.5 to 21 nm by reducing at various temperatures (800 to 1200 K) precursors containing from 4.5 to 23 wt% of nickel. Additional experiments were performed on unsupported nickel powders prepared by reduction of $Ni(OH)_2$, and on reduced nickel antigorite, in which the exposed faces of nickel particles were shown to be (111) planes.

Kinetic experiments were carried out in a quasidifferential flow reactor at atmospheric pressure. The total flow rate was 120 ml/min. Helium was used as a diluent. The propane purity was better than 99.95% (it contains less than 100 and 150 ppm of methane and ethane). No catalyst-aging phenomena were observed at the low propane partial pressure generally used in this work. The formation of reaction products can be considered as resulting from reactions:

$$C_3H_8 + H_2 \rightarrow CH_4 + C_2H_6 \qquad (1)$$

$$C_3H_8 + 2H_2 \rightarrow 3CH_4 \qquad (2)$$

These equations will be written $C_3 = C_1 + C_2$ and $C_3 = 3C_1$. Complete hydrogenolysis of propane into methane can also occur via Reaction (1) and a subsequent ethane hydrogenolysis. This path is assumed to be negligible, as suggested by Shephard (*6*), since ethane is less reactive than propane, as will be confirmed below. The overall reaction will be considered as resulting from both simultaneous Reactions (1) and (2). In what follows, r_1, r_2, and r refer respectively to the rate of propane consumption of Reactions (1), (2), and (1) + (2). The selectivity is defined as $S = r_1/(r_1 + r_2)$.

III. RESULTS

As a first step, the kinetic study of propane hydrogenolysis was performed over the Ni/SiO_2 catalyst previously used (*1*) for ethane hydrogenolysis, referred to as sample A in Table 2 in this paper, over a large range of pressure and temperature. Then, a relation between observed rates and hydrogen coverages was sought.

Kinetic Data

Figure 1 shows that the partial reaction order with respect to propane pressure as a

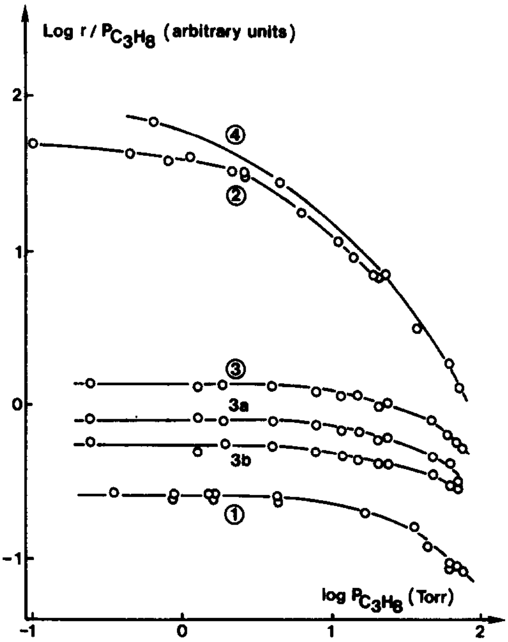

FIG. 1. Sample A: reaction partial orders with respect to propane partial pressure ($n_{C_3H_8} = 1 + s$, s being the slope of the curves). Curve 1, $T = 517$ K, $P_{H_2} = 630$ Torr; curve 2, $T = 517$ K, $P_{H_2} = 63$ Torr; curve 3, $T = 536$ K, $P_{H_2} = 630$ Torr; curve 4, $T = 536$ K, $P_{H_2} = 63$ Torr. curves 3a and 3b correspond to reactions $C_3 = C_1 + C_2$ and $C_3 = 3C$.

function of hydrogen and propane partial pressure. At high hydrogen pressure (P_{H_2} = 630 Torr) and low hydrocarbon pressure ($P_{C_3H_8} \leq$ 7 Torr) the order is equal to unity. It decreases as the hydrocarbon partial pressure increases. Similar conclusions are reached when one considers r_1 and r_2 (curves 3a and 3b). At low hydrogen partial pressure (P_{H_2} = 63 Torr), the reaction order with respect to propane pressure is always lower than unity (curves 2 and 4), and has negative values at large hydrocarbon partial pressures. This seems to be a general feature: a very similar behavior has already been reported in the case of ethylcyclohexane hydrogenolysis over nickel (*7*) and of *n*-hexane over iridium (*8*): at low P_{H_2}/P_{HC} ratio, the partial order with respect to hydrocarbon pressure is negative. It should be noticed that the order with respect to hydrocarbon pressure in the case of ethane hydrogenolysis is higher than unity at high hydrocarbon pressures (*1*), at variance with propane. In what follows, the propane partial pressure is maintained constant at 2 Torr.

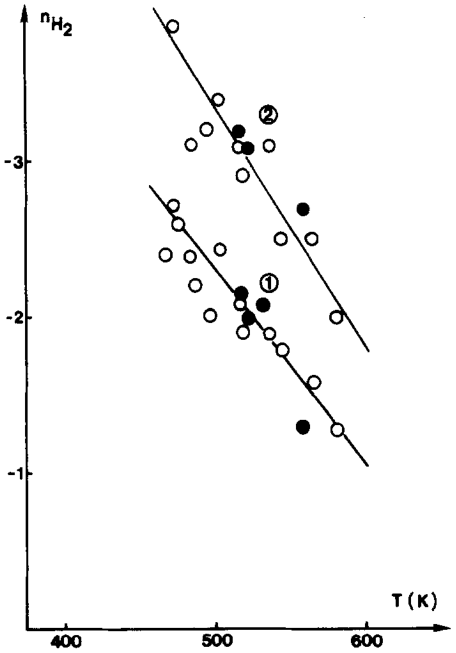

FIG. 3. Orders with respect to hydrogen pressure at P_{H_2} = 600 Torr, $P_{C_3H_8}$ = 2 Torr as a function of temperature. Curves 1 and 2 correspond, respectively, to Reaction (1) ($C_3 = C_1 + C_2$) and Reaction (2) ($C_3 = 3C_1$). Open and filled circles correspond to data obtained on A and B samples.

In Fig. 2 typical variations of conversion rates with hydrogen pressure at a given temperature are shown. The inhibition of Reaction (1) by hydrogen is more pronounced than that of Reaction (2). The orders with respect to hydrogen partial pressure, n_{H_2}, at P_{H_2} ~600 Torr, as a function of temperature T, are shown in Fig. 3 (at this hydrogen pressure, the order for Reactions r_1 and r_2 with respect to propane pressure is equal to unity). It can be seen that n_{H_2} increases with temperature, as already observed by Shephard (*6*) and Guczi *et al.* (*5*) for $r_1 + r_2$.

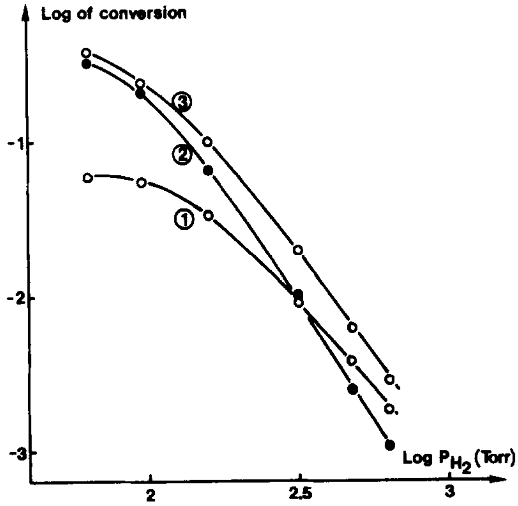

FIG. 2. Log conversion as a function of log hydrogen pressure at 518 K for sample A. The partial hydrocarbon pressure is 2 Torr. Curves 1, 2, and 3, are for Reaction (1) ($C_3 = C_2 + C_1$), Reaction (2) ($C_3 = 3C_1$), and Reactions (1) + (2), respectively.

As already discussed (*1*), in experimental conditions where the partial order with respect to hydrocarbon pressure is equal to unity, the hydrocarbon coverage is probably very small and can be neglected. Degrees of hydrogen coverage in dynamic conditions where the reaction takes place can be estimated from adsorption experiments in a separate apparatus in static conditions. Let us recall (*1*) that for the considered catalyst, the Freundlich law is obeyed (θ_H is proportional to $P^a_{H_2}$, with the exponent a varying with T). Furthermore, we will assume, as in the case of ethane hydrogenolysis, that the relation which holds between r and θ_H is $r = k\theta_H{}^Y(1 - \theta_H)^X$, which is mathematically equivalent to $n_{H_2}/a = Y - X\theta_H/(1 - \theta_H)$ (*1*).

Figure 4 shows the variations of n_{H_2}/a (n_{H_2} from Fig. 3) with $\theta_H/(1 - \theta_H)$. Experimental points are situated on two straight lines whose slopes are 17 ± 3 and 24 ± 3 for Reactions (1) and (2), respectively, going approximately through the origin. This means that orders with respect to hydrogen pressure, and their variations with temperature, are fully accounted for assuming the following rate law:

$$\begin{aligned} r &= kP_{C_3H_8}(1 - \theta_H)^X \\ X_1 &= 17 \pm 3 \text{ for Reaction (1)} \qquad (3) \\ X_2 &= 24 \pm 3 \text{ for Reaction (2).} \end{aligned}$$

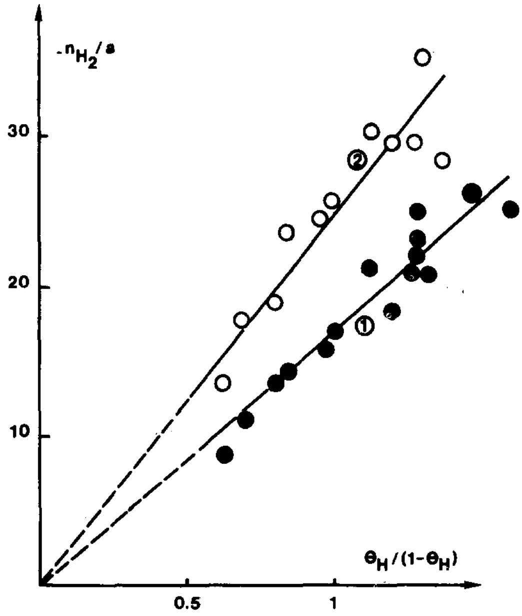

FIG. 4. Parameter n_{H_2}/a for sample A as a function of $\theta_H/(1 - \theta_H)$. n_{H_2}, the order with respect to hydrogen partial pressure, a, the exponent of the Freundlich equation for hydrogen adsorption, and θ_H, the degree of hydrogen coverage: Curve 1, Reaction (1), $C_3 = C_1 + C_2$; curve 2, Reaction (2), $C_3 = 3C_1$.

The apparent activation energy, E_a, is determined by plotting the logarithm of the rate against the reciprocal temperature. At P_{H_2} = 600 Torr, $P_{C_3H_8}$ = 2 Torr and T ~530 K, the apparent activation energies are 47.5 ± 3, 42 ± 3, and 51 ± 3 kcal/mole for reactions r, r_1, and r_2, respectively. As already stated in the case of ethane hydrogenolysis, E_a is a temperature coefficient originating from the variations of k and $f(\theta_H) = (1 - \theta_H)^X$ with T (*1*). It can be written as

$$E_a = E_0 + E_\theta \qquad (4)$$

where E_0 is the true activation energy ($k = k_0 \cdot e^{-E_0/RT}$) and E_θ is defined as $-R = [\partial \log f/\partial (1/T)]_P$.

The true activation energy can be estimated by calculating E_0 from the plot of log $f(\theta_H)$ against $1/T$. A more accurate way to determine E_0 can be used: it can be recalled (*1*) that the apparent activation energy E_a is related to the partial order with respect to hydrogen pressure, n_{H_2}, by the following expression:

$$E_a = E_0 - n_{H_2} \cdot Q \qquad (5)$$

where Q is the isosteric heat of hydrogen adsorption and can be considered, to a first approximation, as a constant nearly equal to 14 kcal/mole (*1*). In experimental conditions where the apparent activation energies are determined, the orders are respectively −1.9 and −3 for Reactions (1) and (2). Hence, one deduces for the true activation energies E_0 the values which are collected in Table 1. This allows us to estimate the equation constant k_0, knowing r in standard conditions, and to compare it with ν, the number of propane molecules colliding with a unit surface area in unit time, as deduced from the kinetic theory of gases (*1*). For both reactions, values thus obtained are summarized in Table 1. The uncertainty in k_0 calculated from uncertainties in E_0 and X values, (±3 kcal/mole and ±3, respectively) is relatively large.

The selectivity $S = r_1/(r_1 + r_2)$ can be

TABLE 1

Values of Parameters in the Rate Expression of Propane Hydrogenolysis $r = k_0 P_{C_3H_8} e^{-E_0/RT} (1 - \theta_H)^X$

Reactions	r^a	X	$E_0{}^b$	$k_0{}^c$	ν^d
(1) $C_3 = C_1 + C_2$	9.1×10^{10}	17 ± 3	14 ± 3	$0.65 \times 10^{22\pm2}$	0.023×10^{22}
(2) $C_3 = 3C_1$	6.6×10^{10}	24 ± 3	9 ± 3	$0.4 \times 10^{22\pm2}$	0.023×10^{22}

[a] Measured at $T = 507$ K, $P_{H_2} = 660$ Torr, $P_{C_3H_8} = 2$ Torr, expressed in molecules/cm²/sec. Average value obtained from four determinations.

[b] In kcal/mole.

[c] In molecules/cm²/sec/Torr.

[d] Number of hydrocarbon molecules colliding with the nickel surface, in molecules/cm²/sec/Torr.

written as:

$$S = [1 + k_{0(2)}/k_{0(1)} (1 - \theta_H)^{(X_2 - X_1)} e^{(E_1 - E_2)/RT}]^{-1} \quad (6)$$

where $k_{0(1)}$ and $k_{0(2)}$ are constants for Reactions (1) and (2).

Its numerical form is:

$$S = [1 + 1.6 (1 - \theta_H)^7 e^{5/RT}]^{-1}. \quad (7)$$

This expression shows that at constant temperature, the selectivity increases with hydrogen pressure. The behavior at constant pressure is more complex. As temperature increases, the selectivity first increases, goes through a maximum, then decreases.

Structure Sensitivity

Most of the results are summarized in Fig. 5 and in Table 2. In Fig. 5 are shown the variations of reaction rate, measured in standard conditions ($T = 507$ K, $P_{H_2} = 160$ Torr, $P_{C_2H_8} = 25$ Torr), with the average nickel particle size, D_{Ni}. For these conditions, it can be seen that the rates of propane and ethane hydrogenolysis vary in a parallel way: the rates ratio $r_{C_3H_8}/r_{C_2H_6}$ is nearly constant and equal to ca. 8. The same value is obtained from data in Table 2 for the unsupported nickel and the reduced antigorite. From data in Fig. 5 and Table 2, it can be seen that the selectivity of propane hydrogenolysis, $S = r_1/(r_1 + r_2)$, is structure insensitive within experimental error ($S = 0.3 \pm 0.05$), as far as the Ni/SiO$_2$ sample with $D_{Ni} = 2.5$ nm is not considered (for this sample, $S = 0.6$). The particular behavior shown by this catalyst is of interest, since the single C–C bond rupture is favored. Further work on more divided nickel catalysts is needed, however, to confirm this tendency.

The dependence of the structure sensitivity of propane hydrogenolysis on temperature and pressure conditions was put to the test in the case of samples A and B (Table 2): the rates ratio r_A/r_B remains approximately constant as hydrogen and propane partial pressures are varied (Table 2). Moreover, at low propane pressures, par-

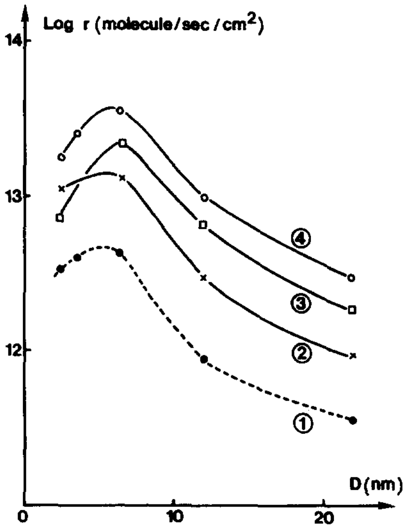

FIG. 5. Log rate of hydrogenolysis at $T = 507$ K, $P_{H_2} = 160$ Torr, $P_{\text{hydrocarbon}} = 25$ Torr as a function of the average nickel particle size. Curve 1, $C_2H_6 + H_2 = 2CH_4$; curve 2, Reaction (1), $C_3 = C_1 + C_2$; curve 3, Reaction (2), $C_3 = 3C_1$; curve 4, Reactions (1) + (2).

TABLE 2

Comparison of Reaction Rates for Various Samples

Samples	Ni loading wt%	$\bar{D}$ (nm)	$r_1{}^a$ ($C_3 = C_1 + C_2$)	$r_2{}^a$ ($C_3 = 3C_1$)	$r = r_1 + r_2{}^a$	$r = r_1 + r_2{}^b$	$r_{C_2H_6}{}^a$
A (Ni/SiO$_2$)	23	6.4	1.3	2.3	3.5	0.015	0.44
B Ni/SiO$_2$	23	21	0.1	0.19	0.29	0.001	0.036
C (reduced antigorite)	45	4–15^c	0.09	0.28	0.37	—	0.04
D (unsupported)	—	67^d	0.9	2.4	3.3	—	0.4

[a] In 10^{13} molecules/sec/cm^2: measured at 507 K, P_{H_2} = 160 Torr, $P_{\text{hydrocarbon}}$ = 25 Torr.

[b] In 10^{13} molecules/sec/cm^2, measured at 507 K, P_{H_2} = 660 Torr, $P_{C_3H_8}$ = 2 Torr.

[c] The sizes of the nickel platelets vary from 4 to 15 nm.

[d] As deduced from the BET surface area.

tial orders with respect to hydrogen pressure are nearly equal for samples A and B (Fig. 3), and apparent activation energies at ca. 540 K have the same values within the experimental uncertainty (±3 kcal/mole). Thus, it can be concluded that the variations of the rate of propane hydrogenolysis with nickel particle size at $D_{\text{Ni}} \geqslant 6.4$ nm do not depend on the temperature and the reactant partial pressure at which the rate is measured, a conclusion which was already reached in the case of ethane hydrogenolysis (*3*, *4*).

DISCUSSION

The rate of propane hydrogenolysis has been shown to be proportional to $(1 - \theta_H)^X$, which is the probability of finding, at least, X adjacent nickel atoms free from adsorbed hydrogen, if the H distribution on the nickel surface is assumed to be random. This suggests that reactive sites are ensembles of X adjacent nickel atoms free from adsorbed hydrogen. This hypothesis has been confirmed in this laboratory: propane hydrogenolysis was studied over silica-supported Ni–Cu alloys (*9*), and for an alloy of surface copper concentration, x, the activity, A_x, was:

$$A_x = A_0(1 - x)^N. \tag{8}$$

Assuming that the short-range ordering of nickel and copper atoms is negligible on the surface, Eq. (8) indicates that the rate is proportional to the probability of having at least N adjacent nickel atoms. As seen in Table 3, N and X values are close together, whatever the considered reaction, thus, confirming the proposed hypothesis. Data on ethane hydrogenolysis (*1*, *9*) are also reported in the table.

In Table 3, X and N values can also be compared to n, the number of nickel atoms involved in the hydrocarbon adsorption at ca. 360 K as a completely dehydrogenated and cracked species (*10*), deduced from magnetic measurements according to:

TABLE 3

Comparison of Exponents X, N, of Corresponding Magnetic Bond Numbers, and of True Activation Energies, for Ethane and Propane Hydrogenolysis

Reaction	X from $(1 - \theta_H)^X$	N from $(1 - x)^N$	n from magnetic methods	E_0 (kcal/mole)
(1) $C_3 = C_1 + C_2$	17 ∓ 3	12 ∓ 2	—	14 ∓ 3
(2) $C_3 = C_3 = 3C_1$	24 ∓ 3	17 ∓ 2	17	9 ∓ 3
(3) $C_2 = 2C_1$	15 ∓ 2	12 ∓ 2	12	14 ∓ 1

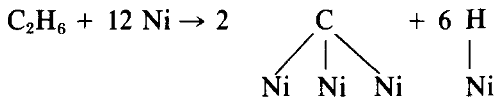 (9)

$$\mathrm{C_2H_6} + 12\,\mathrm{Ni} \rightarrow 2\begin{array}{c}\mathrm{C}\\ /\,|\,\backslash\\ \mathrm{Ni\ Ni\ Ni}\end{array} + 6\begin{array}{c}\mathrm{H}\\ |\\ \mathrm{Ni}\end{array} \qquad (9)$$

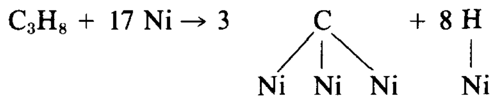 (10)

$$\mathrm{C_3H_8} + 17\,\mathrm{Ni} \rightarrow 3\begin{array}{c}\mathrm{C}\\ /\,|\,\backslash\\ \mathrm{Ni\ Ni\ Ni}\end{array} + 8\begin{array}{c}\mathrm{H}\\ |\\ \mathrm{Ni}\end{array} \qquad (10)$$

For Reactions (2) and (3) in Table 3, X, N, and n are nearly equal. This suggests that intermediates in these reactions are adsorbed species in Eqs. (9) and (10) which require 12 and 17 adjacent nickel atoms.

Magnetic measurements showed no intermediate species corresponding to formation of C_1 and C_2 adsorbed fragments (*10*). This could be explained by the fact that the $C_1 + C_2$ species is not thermostable over a sufficiently large range of temperature to be detected by the thermomagnetic technique (*10*). An alternative explanation is that this species can be formed only in the presence of adsorbed hydrogen. Further experiments are necessary to make this point clearer.

One may speculate on how the $C_1 + C_2$ intermediate is held on the nickel surface with the help of data reported elsewhere (*10*). The adsorbed C_1 species is probably completely dehydrogenated and bonded to three nickel atoms. Hence, a possible model would be,

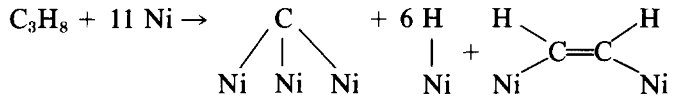 (11)

$$\mathrm{C_3H_8} + 11\,\mathrm{Ni} \rightarrow \begin{array}{c}\mathrm{C}\\ /\,|\,\backslash\\ \mathrm{Ni\ Ni\ Ni}\end{array} + 6\begin{array}{c}\mathrm{H}\\ |\\ \mathrm{Ni}\end{array} + \begin{array}{c}\mathrm{H}\qquad\mathrm{H}\\ \backslash\quad /\\ \mathrm{C{=}C}\\ /\quad \backslash\\ \mathrm{Ni}\qquad\mathrm{Ni}\end{array} \qquad (11)$$

since C_2 hydrocarbons (ethane, ethylene, acetylene) are probably adsorbed in the uncracked form as C_2H_2 radicals bonded to two nickel atoms (*10*). The number of nickel atoms thus required is nearly equal to the corresponding N and X values.

In Table 3, it can be seen that X values are systematically higher than N values. This could be due to some partial ordering of hydrogen atoms on the nickel surface which would lead to too large X values.

The uncertainties in X and E_0 (Table 3) do not allow an accurate determination of k_0. The calculated values are, however, comparable with ν, the number of propane molecules colliding with the nickel surface in unit time, within the rather large experiment uncertainty (Table 1). This result and the fact that at low $P_{C_3H_8}/P_{H_2}$ the partial order with respect to propane pressure is equal to unity, suggest that the rate-limiting step is the irreversible formation of surface species shown in Eq. (10) and possibly (11), in competition with the hydrogen adsorption, as was proposed for ethane hydrogenolysis (*1*).

When $P_{C_3H_8}/P_{H_2}$ is larger, the coverage in hydrocarbon radicals cannot be considered as negligible, as stated by Frennet *et al.* (*11*), and the proposed kinetic equations are no longer valid. A quantitative treatment of these phenomena would require measurements of coadsorbed hydrogen and hydrocarbon coverages in various temperature and pressure conditions.

With regards to structure sensitivity of propane hydrogenolysis, most of the observed results are similar to those previously reported in the case of ethane hydrogenolysis (*3, 4*): the variations of the rate with nickel particle size do not seem to depend on standard conditions at which the rate is measured. Moreover, the rate of propane and ethane hydrogenolysis ratio is independent of the sample morphology for diameters of nickel particles larger than 6 nm. This suggests that active and inactive nickel surfaces are the same for both reactions. Let us recall conclusions reached in the case of ethane hydrogenolysis (*3, 4*), which probably hold for propane hydrogenolysis, namely (i) (111) planes are inactive or, at least, have a very low activity, and (ii) all other surface nickel atoms are nearly equivalent from the viewpoint of activity.

Desjonquères and Cyrot-Lackmann (*12*) have calculated the local density of electronic states (L.D.S.) of surface nickel atoms in the tight binding approximation with the moment method. L.D.S. on nondense surfaces shows a resonant peak of surface states in the middle of the band, whatever their crystalline structure, by contrast with the L.D.S. on infinite dense surface [(111) face in fcc], which is similar to the density of states of bulk nickel. A parallel can be drawn between local electronic properties and catalytic activities: the activity for hydrogenolysis could be related with the presence of the resonant peak in the middle of the band of the density of electronic states.

It is concluded that the model previously proposed for ethane hydrogenolysis is fully capable of accounting for propane hydrogenolysis which involves two parallel reactions, the complete cracking into methane, and the rupture of one C–C bond. The question, now, is to know to what extent the model is applicable to hydrogenolysis over other metals besides nickel and to other reactions.

ACKNOWLEDGMENT

We are indebted to Dr. B. Imelik for very helpful discussions.

REFERENCES

1. Martin, G. A., *J. Catal.* **60,** 345 (1979).
2. Anderson, J. R., *in* "Advances in Catalysis" (D. D. Eley, H. Pines, and P. B. Weisz, Eds.), Vol. 23. p. 70. Academic Press, New York, 1973.
3. Martin, G. A., *J. Catal.* **60,** 452 (1979).
4. Martin. G. A., and Dalmon, J. A., *C.R. Acad. Sci. Ser. C* **286,** 127 (1978).
5. Guczi, L., Sárkány, A., and Tétényi, P., "Proc. Fifth Int. Congress on Catalysis (Florida 1972), p. 1111. North Holland/American Elsevier, 1973.
6. Shephard, F. E., *J. Catal.* **14,** 148 (1969).
7. Kochloefl, K., and Bazant, V., *J. Catal.* **8,** 250 (1967).
8. Boitiaux, J. P., Martino, G., and Montarnal, R., *C.R. Acad. Sci. Ser. C* **280,** 1451 (1975).
9. Dalmon, J. A., *C.R. Acad. Sci. Ser. C* **284,** 821 (1977); Dalmon, J. A., and Martin, G. A., *J. Catal.*, in press.
10. Martin, G. A., and Imelik, B., *Surface Sci.* **42,** 157 (1974).
11. Frennet, A., Liénard, G., Crucq, A., and Degols, L., *J. Catal.* **53,** 150 (1978).
12. Desjonquères, M. C., and Cyrot-Lackmann, F., *Solid State Commun.* **18,** 1127 (1976).